ELSEVIER

Journal of Alloys and Compounds 330–332 (2002) 357–360

Journal of ALLOYS AND COMPOUNDS

www.elsevier.com/locate/jallcom

Thermal diffusivity and electrical resistivity of zirconium hydride

B. Tsuchiya[a,*], M. Teshigawara[b], K. Konashi[a], M. Yamawaki[c]

[a]*The Oarai Branch, Institute for Materials Research, Tohoku University, Oarai-machi, Ibaraki-ken 311-1313, Japan*

[b]*Spallation Neutron Laboratory, Tokai Research Establishment, Japan Atomic Energy Research Institute, Tokai-mura, Ibaraki-ken 319-1195, Japan*

[c]*Department of Quantum Engineering and Systems Science, Graduate School of Engineering, University of Tokyo, 7-3-1 Hongo, Bunkyo-ku, Tokyo 113-8656, Japan*

Abstract

Thermal diffusivity of ε-phase zirconium hydride (ε-ZrH_x: $x=1.74$–1.99) has been measured within the temperature range from room temperature to 600 K. The thermal conductivity of ε-ZrH_x has also been derived from the present experimental data of the thermal diffusivity and the literature data of the specific heat and the density. The electrical resistivity has also been measured to understand the temperature dependence of the thermal conductivity. The comparison between temperature dependencies of thermal conductivity and the electrical conductivity shows that the electronic heat conduction is the dominant process in ε-ZrH_x. Moreover, it is confirmed that the Lorenz number of ε-$ZrH_{1.94}$ for the Wiedemann–Franz rule is 4.0×10^{-2} $\mu\Omega$ W/K^2 in the temperature range of 500–600 K and close to that of Zr metal.

Keywords: ε-phase zirconium hydride; Thermal diffusivity; Thermal conductivity; Electrical resistivity; Electrical conductivity; Lorenz number

1. Introduction

High-level radioactive wastes generated after reprocessing spent nuclear fuels from nuclear reactors include long-lived radioactive nuclides. Recently, the transmutation method using actinide (^{237}Np, ^{241}Am and ^{243}Am)–Zr hydride targets has been proposed to reduce the amount of actinide in nuclear waste [1]. One of the major R&D items to establish the transmutation method is development of the actinide hydride target which can be stably irradiated in reactors. The actinide hydrides easily decompose at the high temperature and increase the internal pressure of target element. The temperature is one of the most important parameters which limit the irradiation of the actinide hydride targets.

The irradiation target consists of several metal phases and hydride phases. The Zr hydride is one of the main components of the hydride target. In this study, the thermal diffusivity of Zr hydride has been studied. The thermal conductivity can be calculated from the measured thermal diffusivity data with the literature data of the specific heat and the density. The electrical resistivity has been also measured for understanding the temperature dependence of the thermal conductivity.

The thermal diffusivity and the electrical resistivity data on Zr hydrides have been measured by Weeks and Bickel et al. [2,3]. However, their data at the high hydrogen concentration and high temperature (above 300 K) have not been reported well yet. In this study, the thermal diffusivity and the electrical resistivity of ε-phase ZrH_x ($1.7<x<2.0$) have been measured at temperatures below 600 K, where no hydrogen is released. In addition, the Lorenz number for the Wiedemann–Franz rule is calculated from the relation of the thermal and electrical conductivities and the heat conduction of ε-phase ZrH_x is discussed.

2. Experiments

2.1. Preparation of ε-ZrH_x

The hydrogenation of Zr was performed by means of a Sieverts apparatus. The dimensions of 99.8 wt.% pure Zr specimens were $\phi10.0\times1.0$ mm^3 for the thermal diffusivity measurement and $1.2\times1.2\times20.0$ mm^3 for the electrical resistivity measurement. The Zr specimen was placed into a quartz vessel in vacuum under a pressure of 4.0×10^{-5} Pa. Fig. 1 shows the hydrogen absorption history for the hydrogenation. After removing a little residual hydrogen in the Zr specimen by heating at 1073 K for 1 h (t_h), the

*Corresponding author. Fax: +81-29-267-4947.

E-mail address: tsuchiya@imr.tohoku.ac.jp (B. Tsuchiya).

0925-8388/02/$ – see front matter
PII: S0925-8388(01)01434-7

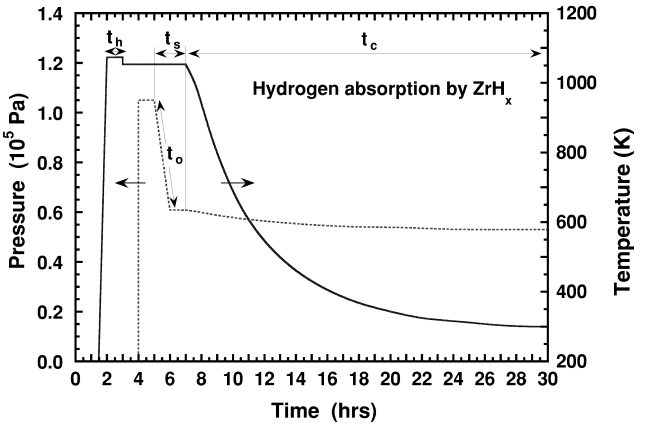

Fig. 1. Hydrogen absorption history for the hydrogenation which was performed using a Sieverts apparatus.

specimens with various hydrogen-to-zirconium (H/Zr= 1.74–1.99) ratios were prepared by adjusting the hydrogen gas pressures of 0.90×10^5 to 1.13×10^5 Pa at 1053 K for 2 h (t_s) and cooled down to room temperature. When the hydrogen gas was induced into the quartz vessel by opening the valve (t_o), the Zr specimen started to absorb hydrogen and the hydrogen pressure rapidly decreased. With the decrease of the temperature, hydrogen was gradually absorbed in Zr (t_c). The scanning electron microscopy (SEM) micrograph of Fig. 2(a) shows microcracks on the surface of the specimens. At the slower rate of cooling, the specimens were successfully prepared without the microcracks, as shown in Fig. 2(b).

The hydrogen concentration was calculated from both the hydrogen pressure changes and mass gains after hydrogenation. The compositions of the specimens were also determined by X-ray diffraction (XRD) and the results were found to agree with the XRD measurement of Cantrell et al. [4]. It was also confirmed from the XRD measurement that the specimens near stoichiometry (H/Zr=2.0) were the ε-phase and had the crystal structure of tetragonal distortion.

2.2. Thermal diffusivity and electrical resistivity measurements

The thermal diffusivity and the electrical resistivity measurements were made using the laser-flash and the four-contact DC methods, respectively. A detailed description of the laser-flash method can be found in Refs. [2,5]. The electrical resistivity measurements were performed in-situ in the Sieverts apparatus after the hydrogenation. The copper wires were welded with the specimens as the four-probe geometry. When the current in the electric field was switched on the outside two probes, the voltage between the inside two probes was measured using a potentiometer. In order to avoid effects of thermoelectric power, the plus and minus voltages (V_+ and V_-) were measured by reversing the electric field. The value of the

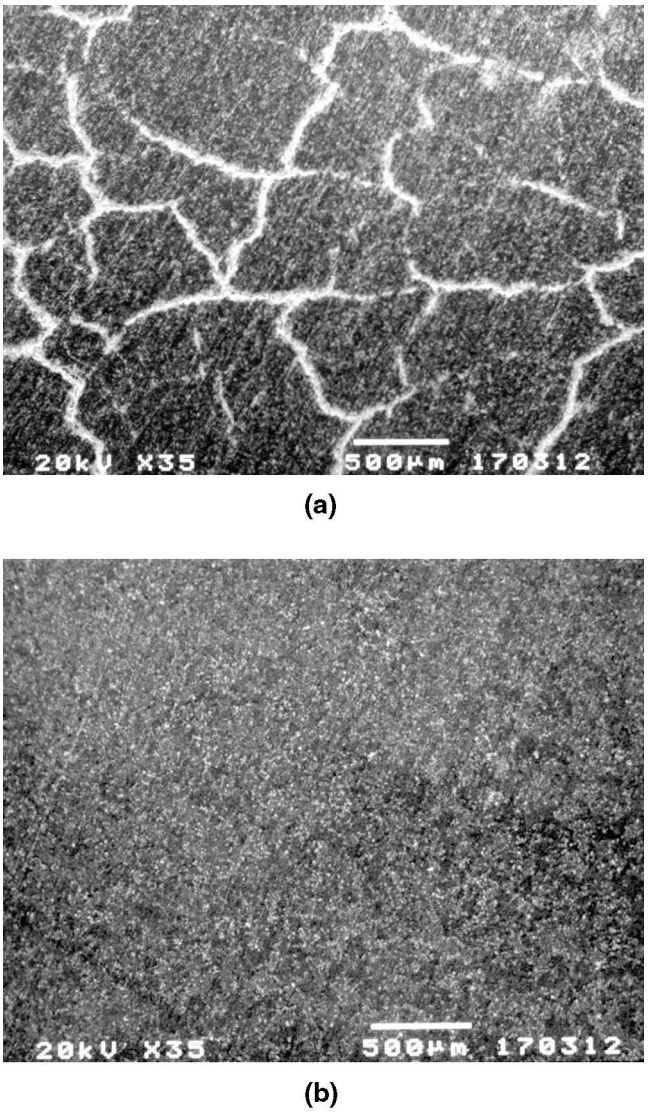

Fig. 2. SEM micrographs (secondary electron image) of $ZrH_{1.94}$ with microcracks (a) and no microcracks (b).

electrical resistivity ρ is calculated by $\rho = VA/Il$, where V is the average voltage ($=(V_+ + V_-)/2$), I is the current, A is the cross-section of the specimen and l is the specimen length between the inside two probes.

For both measurements, the specimen was heated up to 600 K because it has been reported that Zr hydride starts to decompose at temperatures above 700 K quickly [6]. The measurements were reproducible both on heating and cooling the specimen.

3. Experimental results

3.1. Thermal diffusivity

The thermal diffusivities of ε-$ZrH_{1.76}$, ε-$ZrH_{1.83}$, ε-$ZrH_{1.90}$, ε-$ZrH_{1.94}$, ε-$ZrH_{1.96}$ and ε-$ZrH_{1.99}$ are plotted against the temperatures on heating and cooling from room

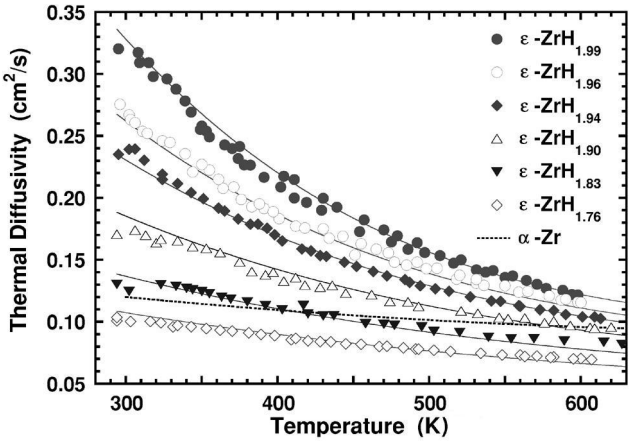

Fig. 3. Temperature dependence of thermal diffusivities for ε-$ZrH_{1.76}$, ε-$ZrH_{1.83}$, ε-$ZrH_{1.90}$, ε-$ZrH_{1.94}$, ε-$ZrH_{1.96}$, ε-$ZrH_{1.99}$ and α-Zr [7]. The solid curves are expressed with Eq. (1), which is obtained by fitting to the experimental data.

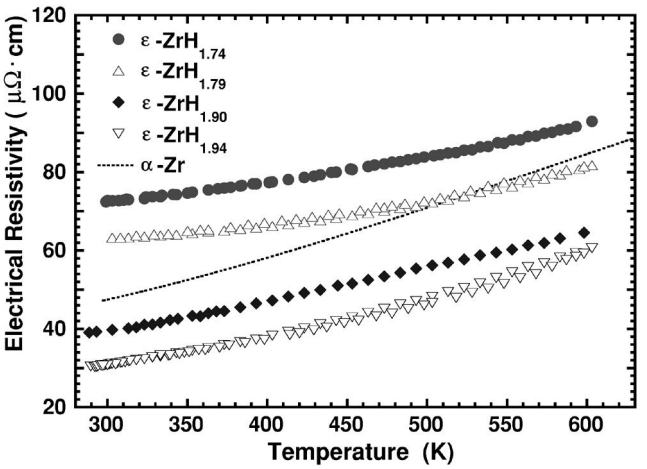

Fig. 4. Temperature dependence of electrical resistivities for ε-$ZrH_{1.74}$, ε-$ZrH_{1.79}$, ε-$ZrH_{1.90}$, ε-$ZrH_{1.94}$ and α-Zr.

temperature to 600 K in Fig. 3. The dashed curve represents that of α-Zr, which has been reported by Takahashi et al. [7]. The data obtained on heating from room temperature to 600 K were consistent with those obtained on cooling. This indicates that the hydrogen release from the specimens during the measurements is negligible. The thermal diffusivity of ε-ZrH_x increases as the x increases and it decreases as the temperature increases. The temperature dependence of thermal diffusivity α (cm^2/s) for different $x = H/Zr$ ratios can be expressed with the following empirical equation which is obtained by fitting to the experimental data;

$$\alpha = \frac{67.9}{\{T + 1.62 \times 10^3 (2.00 - x) - 1.18 \times 10^2\}} - 1.16 \times 10^{-2} \quad (1)$$

where T (K) represents the temperature and the range of x is $1.60 \leq x \leq 2.00$. The thermal diffusivities of ε-ZrH_x for $x = 1.79$, 1.83, 1.86 and 1.91 can be estimated to be equal to that of α-Zr at the temperatures of 300, 400, 500 and 600 K, respectively.

3.2. Electrical resistivity

The electrical resistivities of ε-$ZrH_{1.74}$, ε-$ZrH_{1.79}$, ε-$ZrH_{1.90}$, ε-$ZrH_{1.94}$ and α-Zr (dashed curve) are plotted against the temperatures on heating and cooling from room temperature up to 600 K in Fig. 4. The data obtained on heating were consistent with those obtained on cooling. The electrical resistivities for ε-ZrH_x ($1.74 \leq x \leq 1.96$) at temperatures such as 4.2, 77 and 300 K have been already reported by Bickel et al. [3]. The present data for ε-$ZrH_{1.90}$ and ε-$ZrH_{1.94}$ at 300 K are in good agreement with the reported data. However, there exists a little difference between the present and the reported data for ε-$ZrH_{1.74}$ and ε-$ZrH_{1.79}$. It is also found in Fig. 4 that the ε-ZrH_x ($x \geq 1.90$) is a considerably better electrical conductor than pure Zr metal in the temperature range from room temperature to 600 K.

4. Discussion

4.1. Thermal conductivity

Fig. 5 shows the thermal conductivities for ε-$ZrH_{1.76}$, ε-$ZrH_{1.83}$, ε-$ZrH_{1.90}$, ε-$ZrH_{1.94}$, ε-$ZrH_{1.96}$ and ε-$ZrH_{1.99}$, as compared with that of α-Zr (solid curve) which has been already reported [7]. The values of the thermal conductivity λ for ε-ZrH_x are calculated from the relation $\lambda = \alpha C_p d$, where α, C_p and d are the thermal diffusivity, the specific heat and the density, respectively. The value of α is obtained using Eq. (1). The values of C_p and d for ZrH_x ($x \geq 1.60$) have been already demonstrated to be simple

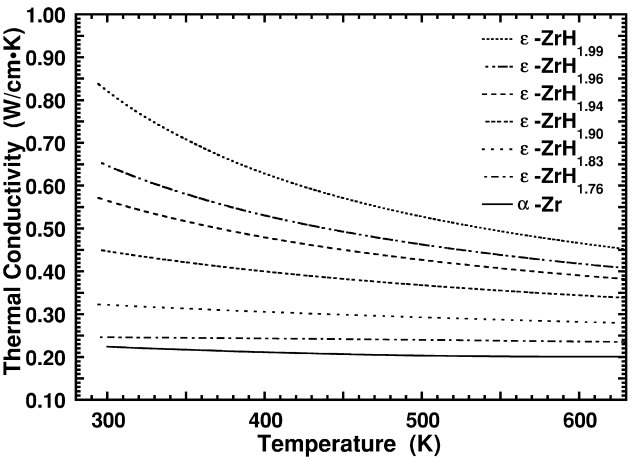

Fig. 5. Temperature dependence of thermal conductivities for ε-$ZrH_{1.76}$, ε-$ZrH_{1.83}$, ε-$ZrH_{1.90}$, ε-$ZrH_{1.94}$, ε-$ZrH_{1.96}$, ε-$ZrH_{1.99}$ and α-Zr [7].

functions of temperature and composition [8]. Fig. 5 shows that λ of ε-ZrH_x decreases as the x decreases and the temperature increases. The temperature and hydrogen concentration dependences of α greatly contribute to those of λ. These results also show that the ε-ZrH_x ($x \geq 1.74$) is a better heat conductor than pure Zr metal within the temperature range of room temperature to 600 K.

4.2. Electrical resistivity and conductivity

The electrical resistivity ρ of ε-ZrH_x is approximately represented with the form of Matthiessen's rule ($\rho = \rho_r + \rho_i$), where ρ_r is the residual resistivity due to impurities (including hydrogen vacancies) and ρ_i is the ideal resistivity due to vibrations of H and Zr atoms. In addition, the resistivity behavior of ρ_i is dominated by scattering of electrons by the acoustic phonons and the optical phonons. ρ_i of ε-$ZrH_{1.74}$, ε-$ZrH_{1.79}$, ε-$ZrH_{1.90}$ and ε-$ZrH_{1.94}$ were obtained by subtracting ρ_r from the present data of ρ. The values of ρ_r of ε-ZrH_x were assumed to be the electrical resistivity at 4.2 K and be expressed with $335(x/2)(1-x/2)$ as a function of H/Zr ratio ($1.6 \leq x \leq 2.0$) according to the Nordheim rule, where $(x/2)$ and $(1-x/2)$ represent the fractions of the H atoms and H vacancies, respectively [3]. It was found that the temperature dependence of ρ_i was similar against several compositions for the ε phase.

The electrical conductivity σ of ε-ZrH_x is represented with $\sigma = 1/\rho$. The temperature dependence of σ corresponds to that of λ. This fact shows that the electronic heat conduction is the dominant process in the ε-ZrH_x. Therefore, the decreases of the thermal diffusivity and conductivity with decreasing the hydrogen concentration and increasing the temperature as shown in Figs. 3 and 5 are ascribed to the electron scattering due to hydrogen vacancy and lattice vibration of Zr and H atoms, respectively.

4.3. Lorenz number

The dependence of the Lorenz number L on temperature T was calculated from the relation $L = \lambda/\sigma T$ for the Wiedemann–Franz rule. The values of L are independent of the hydrogen concentration and gradually decrease as the temperature increases. Particularly, the value of L for ε-$ZrH_{1.94}$ is 4.0×10^{-2} $\mu\Omega\,W/K^2$ at the temperature range from 500 to 600 K and close to that of α-Zr as well. The results indicate that the thermal property of Zr hydride is highly metallic and that its thermal conductance is due to the free electrons.

5. Summary

To understand the thermal properties of ε-ZrH_x, the thermal diffusivity and the electrical resistivity of the ε-ZrH_x were measured in the temperature range of 300–600 K by means of laser-flash and four-contact DC methods, respectively, and the thermal and the electrical conductivities were estimated. The temperature dependence of the thermal conductivity corresponds to that of the electrical conductivity. It is also found that ε-ZrH_x ($x \geq 1.90$) is a much better thermal and electrical conductor than Zr metal within the temperature range of 300–600 K. These results indicate that ε-ZrH_x has a metallic nature and the electrons play a prominent role in the heat conduction of the ε-ZrH_x. Moreover, the Lorenz number of ε-ZrH_x for the Wiedemann–Franz rule was found to be close to those of metals in the temperature range from room temperature to 600 K. It proves that the thermal property of Zr hydride is highly metallic and that the thermal conductance is due to the free electrons.

References

[1] M. Yamawaki, H. Suwarno, T. Yamamoto, T. Sanda, K. Fujimura, K. Kawashima, K. Konashi, J. Alloys Comp. 271–273 (1998) 530.
[2] C.C. Weeks, M.M. Nakata, C.A. Smith, Thermal properties of SNAP fuels, in: Proceedings 7th Conference on Thermal Conductivity, Nov. 13–16, 1967, 1968, p. 387.
[3] P.W. Bickel, T.G. Berlincourt, Phys. Rev. B2 (1970) 4807.
[4] J.S. Cantrell, R.C. Bowman Jr., D.B. Sullenger, J. Phys. Chem. 88 (1984) 918.
[5] W.J. Parker, R.J. Jenkins, C.P. Butler, G.L. Abbott, J. Appl. Phys. 32 (1961) 1679.
[6] J.A. Llauger, G.N. Walton, J. Nucl. Mater. 97 (1981) 185.
[7] Y. Takahashi, M. Yamawaki, K. Yamamoto, J. Nucl. Mater. 154 (1988) 141.
[8] M.T. Simnad, Nucl. Eng. Design 64 (1981) 403.